Syn-diagenetic deformation of a turbiditic succession related to submarine gravity nappe emplacement, Autapie Nappe, French Alps

Pierre Labaume

SUMMARY: The Autapie Nappe (French Alps) consists of a Late Cretaceous 'Helminthoid Flysch' turbiditic succession. It was emplaced in the external Alps during the Late Eocene under the form of a gravity submarine nappe sliding in a turbiditic foreland basin. The syn-diagenetic gravity spreading of the Helminthoid Flysch succession resulted in a pervasive extensional disruption of the sandstone and mudstone layers related to decollements in the marlstone and claystone layers. The deformation regimes and mechanisms testify to: (i) the incomplete and inhomogeneous lithification of the sediments, and (ii) the occurrence of pore pressure gradients and, possibly, excess pore pressure during the deformation. In particular, the critical state of lithification of the sandstone allowed the occurrence of an unusual chronology of deformation mechanisms, the 'brecciation' resulting from a partial loss of cohesion of the sandstone in high speed escaping pore-water (ductile, 'soft-sediment' behaviour) post-dating calcite-filled veins (brittle, 'rock' behaviour). Similar deformation style might be expected to occur at modern convergent margins.

Soft-sediment deformation was first described for syn-sedimentary structures, but it is now known that it can occur under wider conditions (Fitches & Maltman 1978; Maltman 1984, *this volume*). Moreover, since soft-sediment deformation usually affects water-saturated sediments, intergranular water behaviour (migration and possible overpressuring) commonly influences the deformation style. These factors must be considered when the evolution of convergent margin accretionary prisms and submarine nappes is analysed since: (i) these structures usually involve recently deposited sediments; (ii) fluid behaviour is an important parameter of their evolution (Von Huene & Lee 1982; Von Huene 1984). Investigation of modern convergent margins provides direct evidence of active processes such as fluid circulation and overpressuring (Moore *et al.* 1982; Suess & Massoth 1984; Legett & Platt 1985; Boulègue *et al.* 1985), but the study of the geometry and mechanisms of the deformation is difficult there because of the limits of seismic profile interpretation and core and dive observations. On the other hand, the active processes cannot be observed in similar inland ancient series, but their resulting structures can be analysed there. Therefore, the study of these ancient structures may furnish data useful in establishing deformation models for active margins.

This paper is devoted to the Helminthoid Flysch succession of the Autapie Nappe, an ancient submarine nappe of the French Alps. We describe an early stage of extensional deformation and discuss how the deformation features testify to the state of lithification of the sediments as well as the strain and pore-water pressure conditions prevailing during the deformation. The 'state of lithification' will be regarded as the state of achievement of all the processes (compaction and related water escape, pressure solution, recrystallization, cementation etc.) which progressively changed the sediments into rocks, reducing porosity and enhancing cohesion and viscosity.

Geological setting

The Autapie Nappe belongs to a group of allochtonous units which now rest upon the Mesozoic and Eocene sedimentary cover of the external Alps (Dauphinois Zone) between the Argentera and Pelvoux external crystalline massifs (Fig. 1). These thrust-sheets form three principal 'nappes' (Kerckhove 1969): (i) the sub-Briançonnais Units; (ii) and (iii) two Helminthoid Flysch nappes, the Autapie and Parpaillon Nappes.

The Helminthoid Flysch is a Late Cretaceous (locally up to Palaeocene) turbiditic succession and was the last stratum deposited in the Tethyan Ocean (Kerckhove 1969; Debelmas 1975; Kerckhove *et al.* 1981; Caron *et al.* 1981; Homewood & Caron 1982). Its deposition occurred east of the contemporaneous obduction zone of the Tethyan

From: JONES, M. E. & PRESTON, R. M. F. (eds), 1987, *Deformation of Sediments and Sedimentary Rocks,* Geological Society Special Publication No. 29, pp. 147–163.

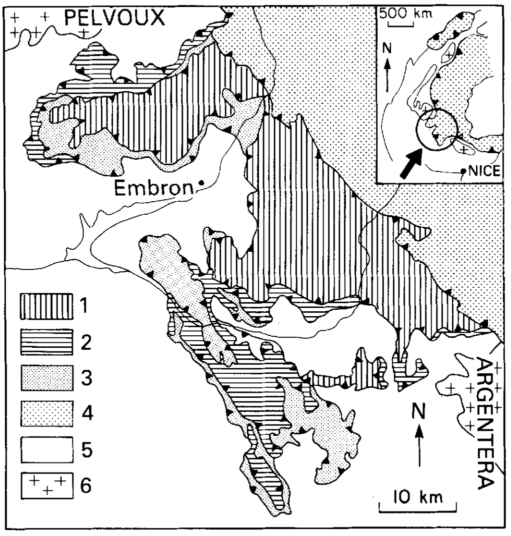

FIG. 1. Geological setting of the Autapie Nappe. 1: Parpaillon Nappe; 2: Autapie Nappe; 3: Sub-Briançonnais Units; 4: Other internal Alps units; 5: Meso-Cenozoic sediments of the Dauphinois zone (external Alps); 6: External crystalline massifs.

oceanic crust above the European continental margin (Piedmont zone) (Tricart 1984; Malavieille *et al.* 1984).

The Autapie Nappe was emplaced during the Late Eocene (Priabonian) in the external Alps (sub-Briançonnais and Dauphinois Zones) as a submarine gravity nappe sliding westwards (or north-westwards) with a frontal olistostrome in a turbiditic foreland basin (Kerckhove 1969; Debelmas & Kerckhove 1973; Kerckhove *et al.* 1978; Kerckhove *et al.* 1981; Caron *et al.* 1981). No metamorphism was associated with the nappe emplacement. During the Oligo-Miocene, the nappe and its substratum were involved in polyphased westward to south-westward vergent thrust and fold tectonics (including the emplacement of the sub-Briançonnais units). The Parpaillon Nappe, also gravity-driven, was emplaced in the area during the Early Miocene (Kerckhove 1969; Merle & Brun 1984).

Lithology

The Autapie Helminthoid Flysch consists of an originally regular succession of plane and parallel turbiditic beds and interlayered hemipelagics (Kerckhove 1969; Sagri 1979; Caron *et al.* 1981).

Four basic lithotypes form three types of beds (Fig. 2):

1 Light-grey massive and strongly lithified calcareous mudstone layers probably deposited by low-density turbidity currents (Te Bouma division).
2 Turbiditic beds displaying usually base-missing Bouma sequences. These fining upward sequences show a basal sandstone layer overlain by a marlstone layer. At the base, the sandstone may be locally coarse to very coarse but is more usually fine to very fine. It consists of siliciclastic grains (mainly quartz grains and minor amount of phyllites, feldspars etc.) and of carbonate bioclasts (mainly pelagic foraminifera). Today, the sandstone is strongly lithified and has a very low porosity, mainly due to carbonate diagenesis (pressure-solution, recrystallization and cementation). The marlstone becomes progressively richer in clay towards the top and it usually presents a layer-parallel fissility.
3 Dark hemipelagic claystone layers showing a layer-parallel fissility.

Bed thicknesses vary greatly from one bed to another (a few centimetres to a few metres). The relative proportion of the four basic lithotypes also varies widely.

These facies associations, as well as the original geometry of the beds, indicate a basin-plain environment for the Helminthoid Flysch deposition. Calcium carbonate-free hemipelagic clay testifies to a deep-sea deposition, below the calcite compensation level [i.e. below 3500–5000 m, according to Hesse & Butt (1976) and Sagri 1979)].

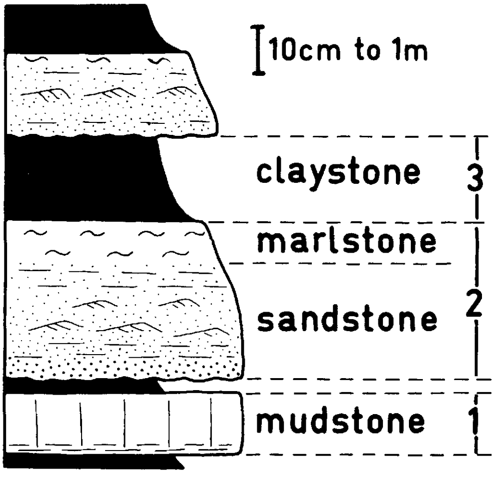

FIG. 2. Bed types and lithotypes of the Helminthoid Flysch of the Autapie Nappe. 1: Low-density carbonate turbidites; 2: Turbidites; 3: Hemipelagics.

Structural style of the deformation stage studied

The polyphased evolution of the nappe is recorded by a complex structure pattern.

An early stage of deformation is characterized by a pervasive stratal disruption resulting from multidirectional extension parallel to the layering (Fig. 3): at the outcrop scale, extensional ramps (normal faults) cut the sandstone and mudstone layers and flatten upwards and downwards as decollements in the marlstone and claystone layers (Fig. 4). Beds, or groups of beds, are thus truncated in lens-shaped, fault-bounded blocks of centimetric to decametric scale. There is no oblique cleavage associated with these structures.

Variations in the stratal disruption intensity led Kerckhove (1969) to define in the nappe three basic deformation facies corresponding to increasing disruption, the 'normal', 'dissociated' and 'ultra-dissociated' facies, respectively. However, many bed ruptures also occur within the normal facies itself. These variations are spatially very closely related to the marlstone and claystone ratio: the parts of the succession poor in marlstone and claystone are relatively weakly deformed; on the other hand, the parts rich in marlstone and claystone are intensely disrupted and show important offsets along the shear planes (in many cases more important than the outcrop dimensions, so that the finite extension usually cannot be measured) locally resulting in a 'block-in-matrix' or 'melange' texture (dissociated and ultra-dissociated facies, Fig. 3). Because of the geometry of the deformation and of the monogenetic constitution of the succession, there is no doubt that this block-in-matrix geometry results from intense shearing and is not of sedimentary origin (olistostrome) (Hsü 1974).

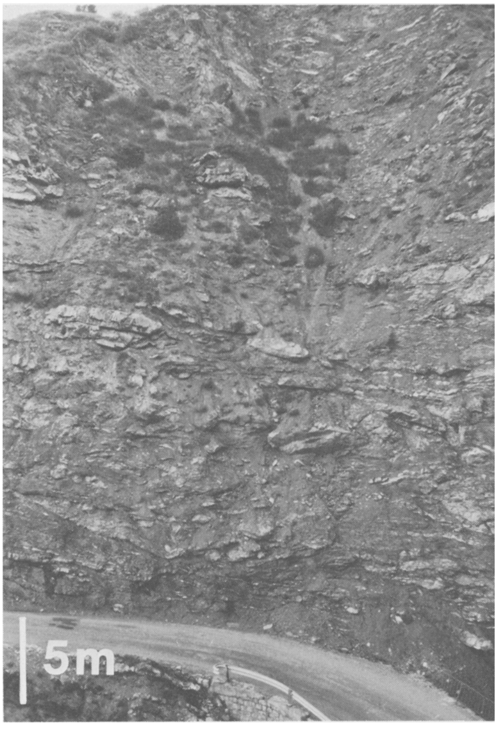

FIG. 3. Typical outcrop of the Autapie Nappe, showing pervasive extensional stratal disruption.

Structures in the sandstone layers

Three types of microstructures may be associated with the extensional ramps cutting the sandstone layers: normal microfaults, calcite-filled veins and 'breccia' (Figs 4 and 5). All of these correspond to layer-parallel extension and layer-normal shortening. They can be formed up to some decimetres from the ramps and progressively disappear further away (Fig. 4). Hereafter, we describe and discuss these various microstructures and then examine their geometrical and genetical relationships.

Calcite-filled veins

Most of these veins (b in Fig. 5) are set at high angles to the bedding. They display a fibrous calcite-fill, indicating layer-parallel extension. The veins are very thin, usually less than 1 mm wide, exceptionally up to 5 mm. The vein opening very rarely induced breakage of grains, but rather occurred by grain to grain separation. Some grains have been completely separated from their neighbours and are isolated in the calcite fill. For this reason, some veins appear locally more like zones of diffuse increase of intergranular calcite cement than like well defined veins.

These features suggest that the sandstone lithification was incipient when the veins developed: grain contact strength (resulting from compaction and probably from incipient cementation) was strong enough for the sand to behave as a cohesive and brittle material, but weak enough for the vein opening to be easier by grain to grain separation than by grain breakage.

Microfaults

These microfaults (a in Fig. 5) usually show a dip of 45°–60° with respect to the layering and induced millimetric to centimetric offsets. Faults are either synthetic or antithetic to the extensional ramps. Faults rarely occur alone but usually

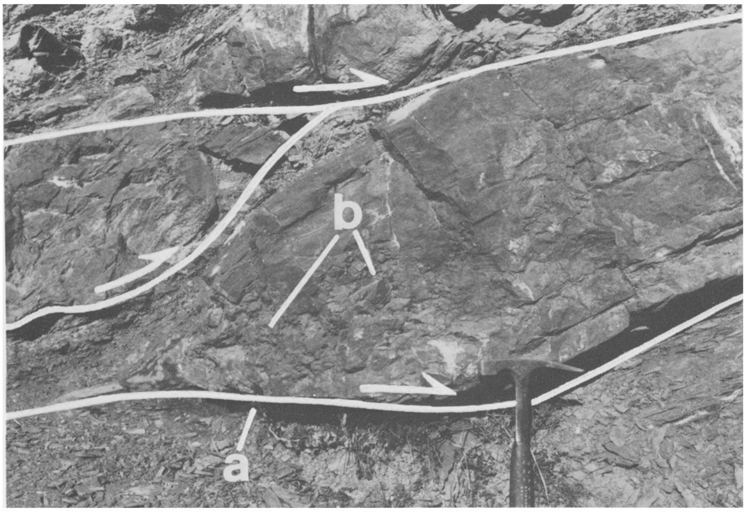

FIG. 4. Sandstone layers cut by extensional ramps (a). Note the breccia-like deformation (b) associated with layer rupture along one of the ramps.

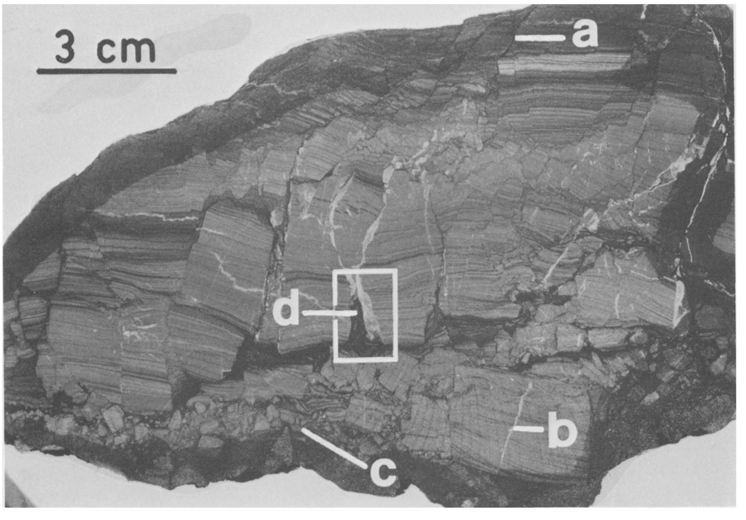

FIG. 5. Deformed sandstone layer showing association of genetically related different types of microstructures (large-size thin section). (a) Microfaults; (b) pre-breccia calcite-filled vein; (c) breccia; (d) sand dyke formed during the brecciation (frame: Fig. 11). The sandstone becomes progressively finer and more phyllite-rich towards the top of the layer.

constitute anastomosed networks with millimetric to centimetric spacing of individual faults. A fault across a sandstone layer consists of a deformation band 0.1–2 mm wide and does not display a discrete slip plane. On the other hand, where a fault separates the sandstone layer from marlstone or claystone, the sandstone surface displays a striated slickenside.

Deformation bands

Fig. 6 shows a deformation band 0.5 mm wide which induced an 8 mm offset. Outside the band, the long axis of grains lies parallel to the bedding. Inside the band, most of the elongated grains have been reoriented parallel to the band walls (a in Fig. 6), evidencing deformation by important grain to grain movements. Progressive reorientation of these grains (particularly in folded phyllites, b in Fig. 6) close to the band walls resulted in a shear zone geometry for the band and indicates the sense of movement. Inside the band, small grains are more abundant than in the

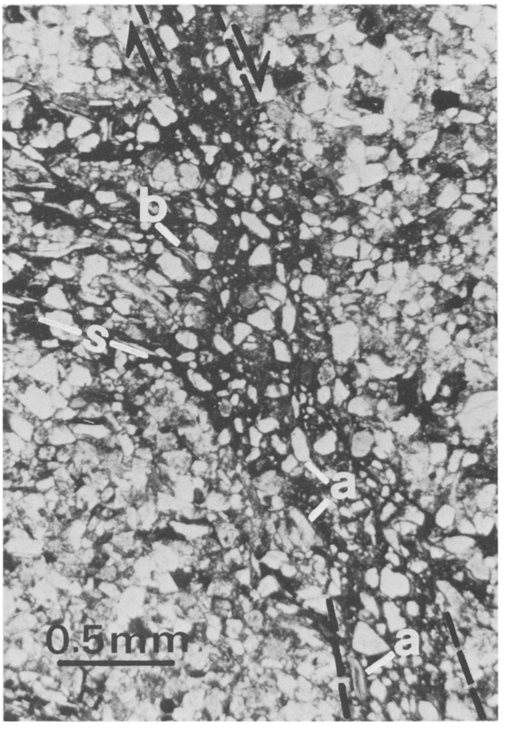

FIG. 6. Deformation band (microfault) in sandstone (thin section). a: reoriented elongated grains; b: folded phyllite; s: layering. Dark colour of the band results from post-faulting alteration by clay minerals.

undeformed sand, and calcite grains are rare. This suggests that intergranular movements were accompanied by grain cataclasis, mainly undergone by the calcite grains. This assumption is supported by the observation of some cracked grains outside the band. The band is brown in colour, due to a later alteration with the development of clay minerals.

Another deformation band, 0.5 mm wide and with a centimetric offset, is shown in Fig. 7. In this case, the grain size reduction by cataclasis inside the band was more intense than in the previous case and very few large grains remain. In particular, no calcite crystal can be found inside the band. Between the grains, a 'dirty', dark and optically irresolvable matrix is probably made of the smallest siliciclastic grain fragments and the completely crushed calcite grains. Outside the band, many cracked grains can be found, crack abundance increasing towards the band walls.

These deformation bands can be considered as ductile faults, the sandstone ductility primarily corresponding to the relative displacements and reorientation of grains or grain fragments. This indicates that the grain contact strength was weak and thus the faults formed in un- or poorly-lithified sediments. Similar natural deformation bands have been described by Aydin (1978), Cowan (1982), Aydin & Johnson (1983), Petit & Laville (*this volume*) and Underhill & Woodcock (*this volume*), who reached analogous conclusions. These conclusions are well supported by the strong analogy existing between the natural structures and those obtained experimentally both in: (i) unlithified sand (Borg *et al.* 1960; Friedman *et al.* 1980) or other granular material (Mandl *et al.* 1977) and (ii) in partly cemented porous sandstone (Handin *et al.* 1963; Dunn *et al.* 1973).

From these experiments, the grain cataclasis is thought to result from stress concentration at grain contacts. Therefore, its intensity would be representative of the intergranular strength opposed to the grain to grain movements and is principally controlled by:

1 The effective confining pressure, which is the difference between the confining pressure carried through the rock (burial) and the pore fluid pressure, as established by Terzaghi (1943) and applied to rock fracturing by Hubbert & Willis (1957), Hubbert & Rubey (1959) and many others. Handin *et al.* (1963) have shown that effective confining relief (i.e. pore pressure increase under constant burial or burial relief under constant pore pressure) tends to reduce cataclasis and to limit it to the deformation band.
2 The porosity. Dunn *et al.* (1973) have shown that high porosity (i.e. weak lithification) also tends to reduce cataclasis and to increase the deformation band width.

Therefore, the weaker cataclasis in the case of the microfault of Fig. 6 than that in the case of Fig. 7 may be due to a lower burial, a higher pore pressure or a weaker lithification. Nevertheless, it may also be due, all other things being equal, to the larger amount of: (i) calcite grains which preferentially underwent cataclasis because of their strength being inferior to that of quartz grains, thus 'protecting' the latter, and (ii) phyllites which acted as a 'lubricant', facilitating the intergranular movements along their borders.

Slickensides

The slickensides exhibit characteristic features (Fig. 8):

1 They are usually undulated.
2 They are rough, with the same weathering aspect as the non-deformed sand. Nevertheless,

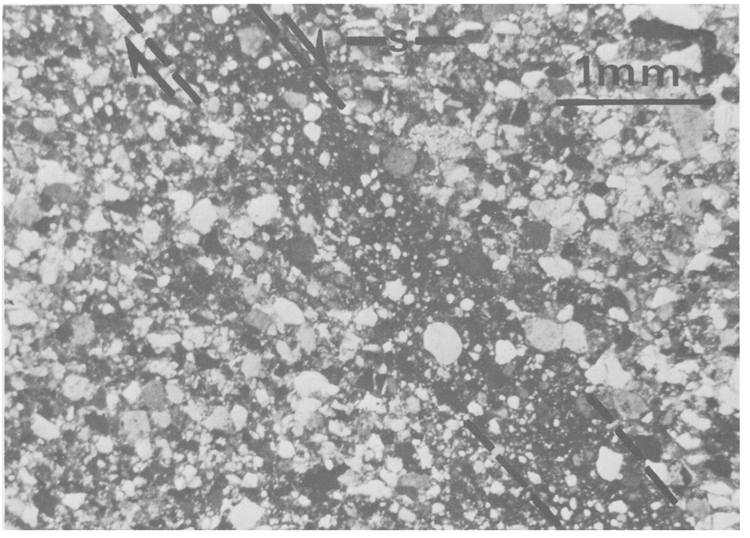

FIG. 7. Deformation band (microfault) in sandstone (thin section). s: layering. Note the strong grain size reduction by cataclasis inside the band.

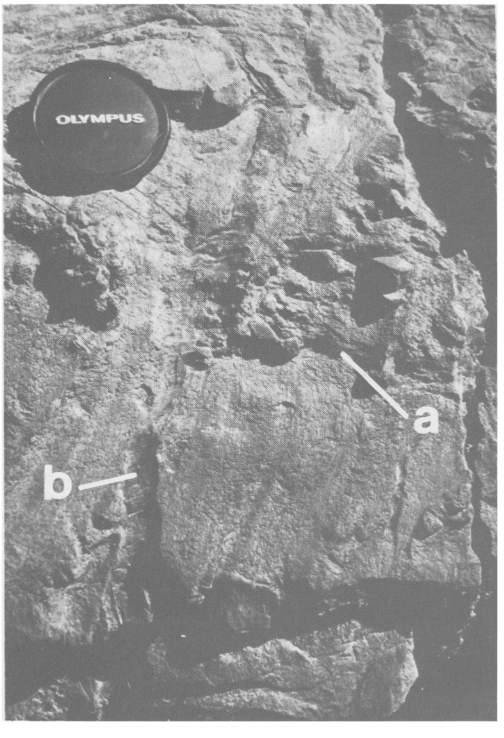

FIG.8. Slickenside in sandstone. (a) Riedel-like shear plane giving the sense of movement (the missing block was moved upwards; note the brecciated texture of the hanging-wall); (b) claystone-filled vein.

locally, they may display a glossy aspect resulting from the spreading of phyllites on the fault plane during faulting.

3 There are no synkinematic fibres of calcite or quartz.

4 Striae indicating the direction of movement consist of grooves, often curved, of millimetric width developed in the sand itself.

5 The sense of movement is given by secondary shear-planes (Riedel planes) and by asymmetric grooves associated with dragged grains. The hanging-walls of the Riedel planes usually present rounded and irregular, locally breccia-like (a in Fig. 8), geometries.

In thin section perpendicular to a slickenside, the fault in the sandstone appears as half of a deformation band, the slickenside being in the deformed sandstone. The Riedel structures also consist of deformation bands.

These slickenside features are probably related to ductile deformation of the sandstone by grain to grain movements associated with slip along the slickensides. Therefore, these features would be specific to faults developed in un- or poorly-lithified sediments. Laville & Petit (1984) and Petit & Laville (*this volume*) have described similar slickensides formed in unlithified fluviatile sandstone. Such faults can easily be discriminated from those developed in strongly lithified sandstone, which are characterized by plane slickensides exhibiting a polished aspect resulting from grain abrasion, synkinematic fibrous crystallizations and sharp geometry of the Riedel planes (Petit *et al.* 1983).

The deformation bands across sandstone do not display slickensides because, in this case, the movement along the fault was only accommodated by ductile deformation in the width of the band, without loss of cohesion along a discrete slip plane. Such rupture planes were only initiated where the faults separated the sandstone layers from adjacent marlstone or claystone layers. Aydin & Johnson (1983) have noted that slip surface initiation inside a deformation band across porous sandstone (i.e. 'change in the style of deformation from continuous and zonal to discontinuous and planar') occurred only when displacement along the fault was of large (metric) amplitude.

Breccia

Breccia corresponds to a more complex and penetrative deformation associated with extensional ramps than the deformation induced by the microfaults.

At the outcrop, the boundary of the deformed layer exhibits sandstone 'clasts' of millimetric to decimentric size, in many cases in relief, in a sandstone 'matrix' (c in Fig. 9). Usually, marlstone or claystone has flowed between the clasts and, at very deformed layer boundaries, some clasts or groups of clasts have been separated from the layer itself. Such deformation is difficult to analyse at the outcrop, because of its chaotic geometry and, locally, because of the diffuse transition between sandstone and marlstone or claystone.

In thin section, one can see that the clasts are formed by sand in which sedimentary laminations have been preserved (c in Fig. 5 and Figs 9 and 10). Although the clast shape can be irregular, many of them are subrectangular, with borders respectively subperpendicular and subparallel to the bedding. Clasts are usually rounded with either sharp or more diffuse borders. Internal layering of the clasts indicates, for some of them, important body rotation; some elongated clasts have been folded.

Around the clasts, the matrix corresponds to sand deformed mainly by grain to grain movements: all sedimentary structures disappeared and shear movements occurred, as indicated by the local preferred orientation of elongated grains. Evidence of quartz grain cataclasis is very rare; on the other hand, cataclasis of calcite grains occurred, as calcite grain size is usually reduced in the deformed sand and foraminifera truncated at clast borders have been observed. Geometrical and compositional relationships between clasts and matrix show that the latter is originated from both the loss of cohesion of the immediately adjacent clasts and from the injec-

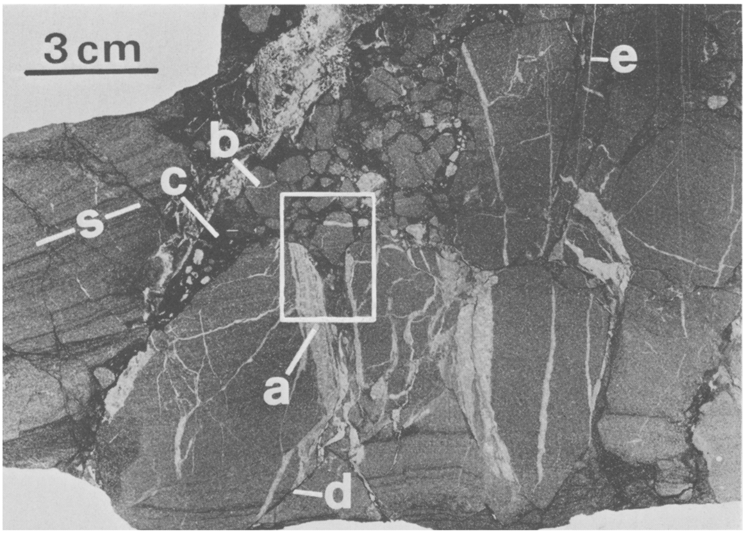

FIG. 9. Early calcite-filled veins and later breccia in sandstone (large-size thin section). a: pre-breccia calcite-filled vein opened and injected with sand during the brecciation (frame: Fig. 10); b: clast of undeformed sandstone; c: matrix of sandstone deformed by grain to grain movements (its dark colour is due to post-breccia pressure solution of calcite and alteration by clay minerals); d: microfault related to the opening of the vein a; e: post-breccia calcite-filled vein; s: layering.

tion between the clasts of sand issued from more distant (up to some centimetres) disaggregated internal layers of the bed. Such injections gave 'sand-dyke' geometries, as shown in Fig. 11, where the injected sand originated from a thin phyllite-rich layer interbedded between thicker phyllite-poor layers. The injected sand shows a strong fabric of grain long-axis, parallel to the dyke borders. Close to the dyke borders, the enclosing sand locally shows disorganization and progressive disappearance of the layering, evidencing incipient brecciation by *in situ* grain mobilization (b in Fig. 11). The deformed sand of the breccia matrix is usually brown in colour, thus darker than the undeformed sand. This is due to strong post-breccia pressure-solution of calcite and alteration with development of clay minerals.

These features suggest that the lithification was weak enough to allow a loss of cohesion of part of the sandstone, but strong enough to allow the preservation of the clasts. The lithification was also inhomogeneous inside individual beds, since the sand of some internal layers was completely mobilized, while large clasts were preserved in others. As in the case of the microfaults, occurrence of phyllites played a major role in facilitating the grain mobility (i.e. sand dyke of Fig. 11). The grain size was also an influential parameter, as shown by the increased brecciation intensity linked with the grain size increase illustrated in the lower part of the layer

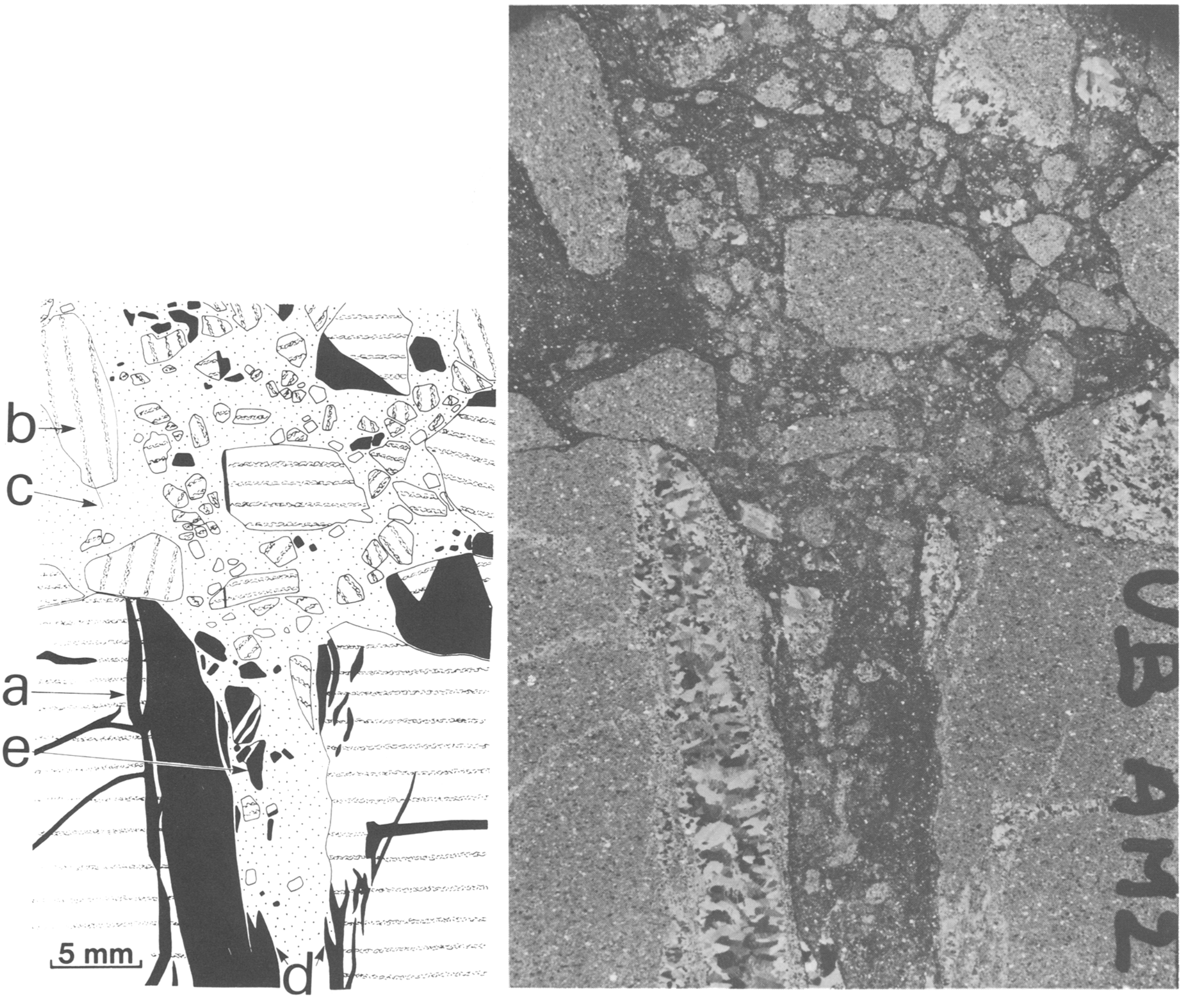

FIG. 10. Early calcite-filled veins and later breccia in sandstone (thin section, situation in Fig. 9). a: pre-breccia calcite-filled vein; b: layered sandstone clast; c: matrix; d: both sides of the same vein, opened and injected by the matrix; e: calcite clast torn away from the neighbouring vein-fill during the matrix flow.

in Fig. 5. This was probably due to a lower volume of intergranular pores and a higher number of grain contacts in the finest sandstone, facilitating, in the latter, a more rapidly efficient lithification.

Sand injections are likely to result from fluidization [grain transport by high-speed escaping pore fluid (Lowe 1976)], implicating pore-water pressure gradients and high strain rate. This suggests that both these parameters controlled the partial loss of cohesion of the sandstone characterizing brecciation.

Microstructure relationships and deformational sequence

The time and space relationships between the microstructures described above indicate the following chronological sequence: (i) normal microfaults and calcite-filled veins; (ii) normal microfaults and breccia. During the first stage, the calcite-filled veins never constituted *en-échelon* precursor sets to the microfaults but, in many cases, they corresponded to a layer-parallel opening at the tip of microfaults. During the second stage, many clast borders and sand injections were initiated by rupture along early calcite-filled veins.

These relationships are well illustrated by Figs 9 and 10, where the opening of a vein (a in Fig. 9) was related to the slip along a fault (d in Fig. 9). The first stage of the vein opening was accompanied by calcite crystallization, and the second by sand injection during the brecciation. During the latter stage, some calcite crystals, or groups of crystals, tore away from the vein-fill and were incorporated into the flowing sand as clasts (e in Fig. 10); some of them underwent cataclasis during this process. Many other remains of early calcite-filled veins can be found in the breccia, either across clasts, at clast borders, or as isolated crystals, or groups of crystals, in the matrix (black in Fig. 10).

Another example of microstructural association is given in Fig. 5, where a set of normal faults developed in the upper part of the sample while breccia occurred at the base, with increasing intensity towards the bottom. In the transitional medium area, early calcite-filled veins were reactivated as faults during the brecciation. These veins were formed subperpendicular to the bedding and later shear movement along them was accompanied by rigid body rotation of the microlithons. The sand dyke of Fig. 11 was formed during the brecciation along one of these early veins; calcite-fill cataclasis during the sand injection occurred, as in the case presented in Fig. 9. Some remains of an early calcite-filled vein are also found in the intensely brecciated lower part. On the other hand, no early veins can be found in the upper part, where only faults developed. We can thus infer a two-stage deformation: layer-parallel extension was accomodated: (i) in the upper part by normal faulting during the whole deformational sequence, and (ii) in the lower part by calcite-filled vein opening during the first stage of deformation and by brecciation during the second one. This second stage induced more important finite extension than the first one.

These vein/breccia relationships, as well as the common clast geometry (borders subparallel and subperpendicular to the bedding), suggest that brecciation was initiated as tensile layer-parallel extension in continuity with opening of the previous calcite-filled veins, but with a drastic change in the deformation mechanisms. This change consisted of a partial loss of cohesion of the sandstone between the two stages, probably resulting from an increase in strain rate inducing pore pressure gradients: with high strain rate, calcite crystallization could not follow the vein opening any longer; this would have induced a relief of the horizontal confining, as well as the pore pressure in the opening zones, thus draining intergranular water towards them. In the less lithified sandstone, this resulted in immediate vein wall disaggregation and collapse; where the cohesion was strongest (particularly where the opening was along early calcite-fill giving rigidity to the walls), actual openings allowed injections of grains from adjacent areas. As deformation continued, shear movements occurred in the matrix, inducing important body rotations of the clasts and cataclasis of the calcite grains. This in turn helped to 'erode' the clasts which were rounded and reduced in size while the matrix developed. This resulted in the complex brecciated texture with abundant matrix and largely occulted initial rupture geometry.

This vein/breccia succession gave an unusual chronology of deformation mechanisms, since brecciation can be referred to as partially ductile, 'soft-sediment' behaviour while the early calcite-filled veins indicate brittle behaviour, classically characteristic of 'rock deformation'.

The distribution of shear and tensile structures is usually not random: Fig. 5 shows that the microfaults preferentially developed in the phyllite-rich layers, and the tensile microstructures in the phyllite-poor layers. This may be due to a higher tensile strength and a lower shear strength of the former than of the latter: as shown in Fig. 12, the shape of the failure envelope of the phyllite-rich sandstone probably tends toward that of a shale (De Sitter 1966, fig. 14). In

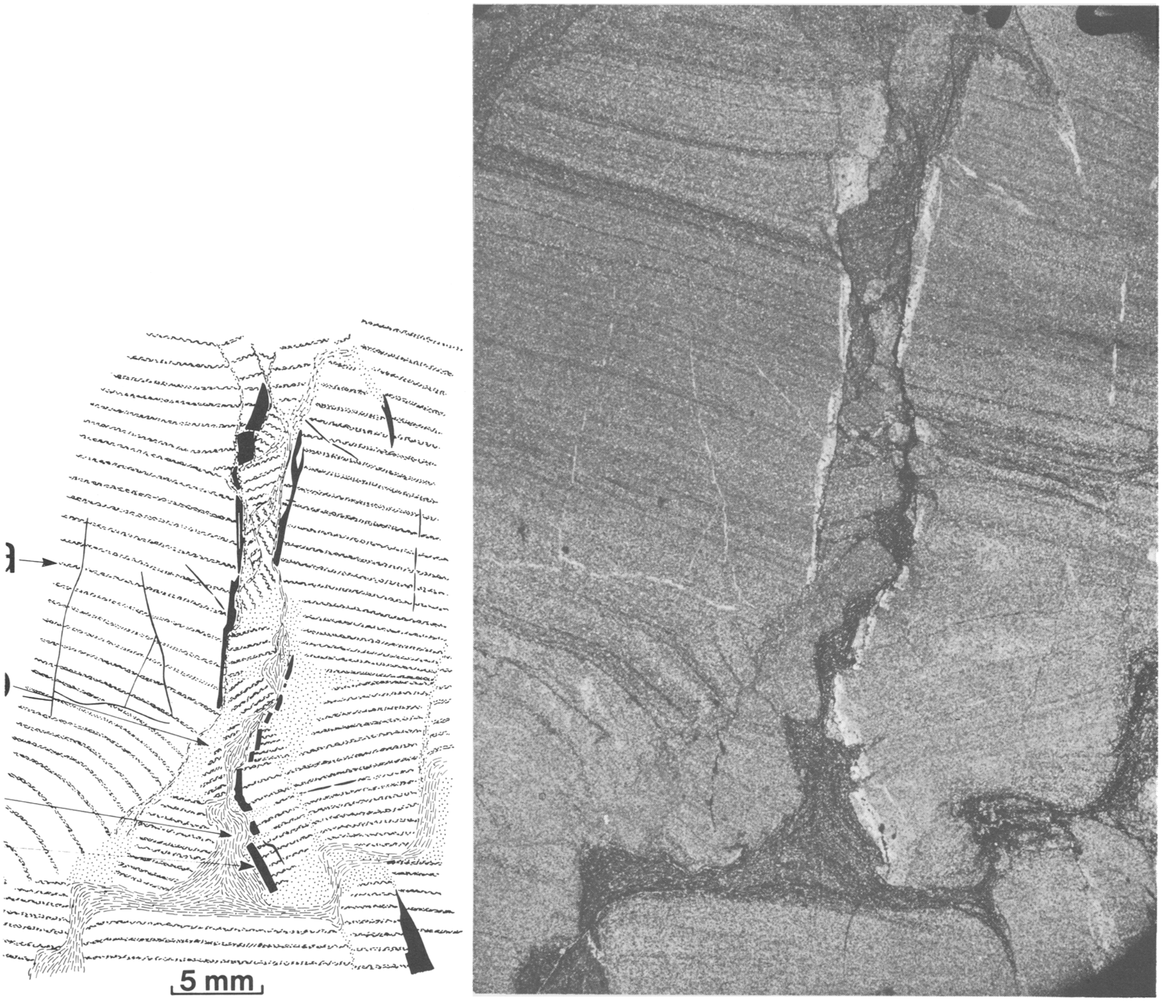

FIG. 11. Upward injection structure (sand dyke) of phyllite-rich sand formed along early calcite-filled veins during the brecciation (thin section, situation in Fig. 5). a: phyllite-poor undeformed layered sandstone; b: sandstone affected by grain to grain movements in the enclosing sandstone of the sand dyke and veins; c: upward injected phyllite-rich sand; d: early calcite-filled vein broken during the injection.

consequence, for a given state of stress, rupture could occur in the shear field for the phyllite-rich sandstone (A in Fig. 12) and in the tensile field for the phyllite-poor sandstone (B in Fig. 12). Since the influence of the phyllite grains consisted of facilitating grain movements along their borders, such control of the sandstone behaviour indicates a weak state of lithification when the deformation occurred.

In conclusion, all microstructure features in the sandstone indicate a weak lithification state at the deformation time. They suggest that early cementation was probably already achieved, but was weak enough to be locally broken, its breakage being easier than that of the grains themselves. This allowed granulometric and compositional variations to firmly control the sandstone behaviour (i.e. the fault-tensile structure distribution, the cataclasis intensity inside the deformation bands and the intensity of the grain mobility during the brecciation), even where these variations are weak (Fig. 5). Completely unlithified sand would probably have undergone more complete grain mobilization, while strongly lithified sandstone would show no grain mobilization and poor influence of the sand composition. This latter point is well illustrated by the later structures of the nappe (see below). The deformation mechanisms also indicate the occurrence of the role played by pore-water. We

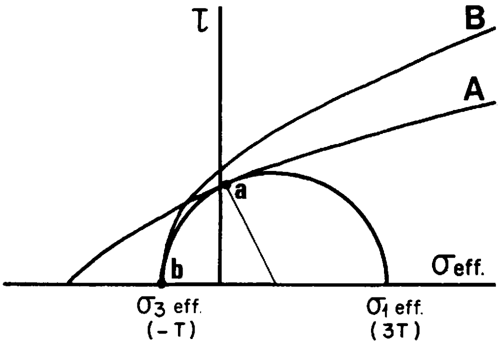

FIG. 12. Possible envelopes of phyllite-rich (A) and phyllite-poor (B) weakly lithified sandstones. For a given state of stress (Mohr circle), rupture occurred in the tensile field for the latter (b) and in the shear field for the former (a). σ_1 eff and σ_3 eff: greatest and least principal effective stresses, respectively; T: tensile strength of the phyllite-poor sandstone.

have discussed how changes of the effective confining pressure (i.e. of pore pressure or of burial) and of the strain rate may have influenced the deformation mechanisms in addition to the influence of the lithological variations. Nevertheless, since all these parameters were likely to vary both in time and space throughout the nappe, an accurate determination of their respective influence remains speculative.

Structures in the mudstone layers

In contrast to the sandstone layers, the mudstone layers present, almost everywhere, a strongly brittle behaviour. The normal faults display synkinematic fibrous calcite crystallization. The calcite-filled vein networks are strongly developed near to the extensional ramps, giving a brecciated texture to the bed (Fig. 13). Except for one observed case, the calcite-filled veins are never post-dated by mud flow and the clasts are always angular in shape. These features indicate that, unlike the sandstone, lithification of the mudstone was advanced when the deformation occurred.

Although the vein network geometries can be complex, the vein opening basically corresponds to layer-parallel extension. As in the case of the sandstone layers, many veins teminate along shear-planes, the vein opening being related to slip along them. Some of these shear-planes are oblique with bedding normal faults but most of them are parallel to the bedding plane (b in Fig. 13). Layer-normal shortening was thus reduced and no related pressure-solution (stylolitization of the bedding planes) was observed.

Figure 14 illustrates a case in which a vein network in mudstone was injected by sand and clay grains originating from neighbouring siliciclastic layers, the injection having probably occurred during brecciation of the latter. This injection is thus similar to those presented in Figs 10 and 11, but, in this case, it did not remain internal to the original bed. The calcite fill of the veins was broken during the injection and many calcite crystals, or groups of crystals, have been integrated into the injected sediment; although some mudstone clasts remained angular in shape, they were also probably partially disaggregated (mud flow), since some of them are rounded, and the injected sediment is rich in carbonate mud. This example emphasizes: (i) the role of pore-water pressure gradients which induced intergranular water movements fluidizing unlithified sediments, and (ii) the difference of lithification state between the mudstone and the sandstone during the deformation.

Marlstone and claystone layers

The marlstone and claystone layers acted as decollement levels while the sandstone and

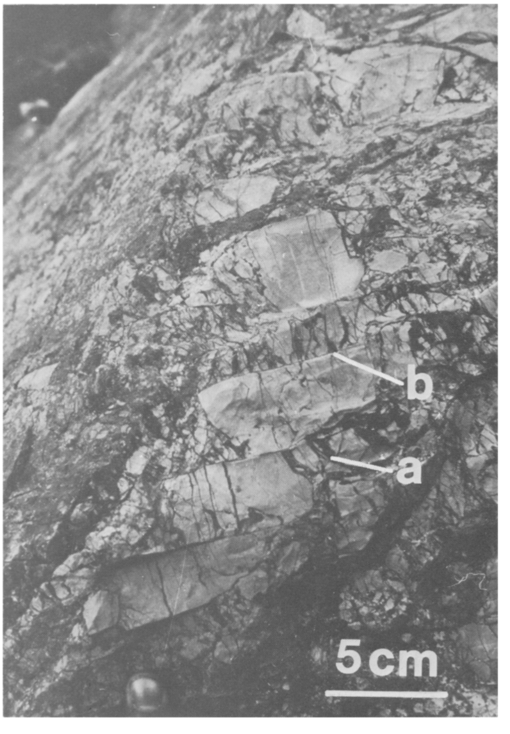

FIG. 13. Calcite-filled vein network (a) giving a brecciated texture in a mudstone layer. b: layering, which acted as decollement levels.

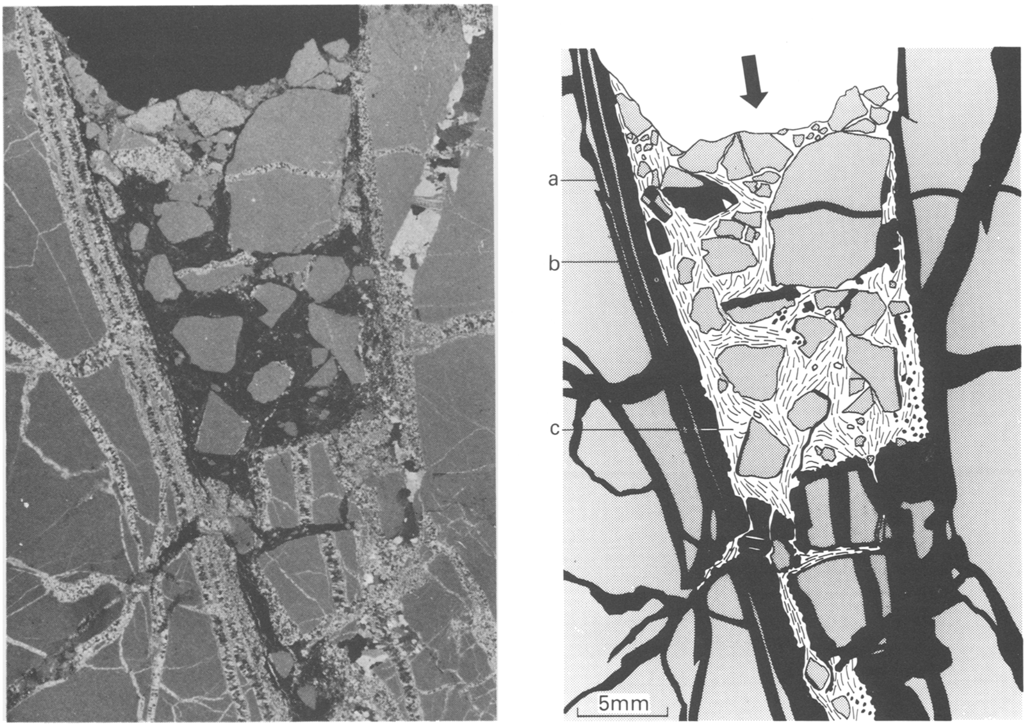

FIG. 14. Sand and clay grain injection structure formed in a calcite-filled vein network in a mudstone layer (thin section). a: mudstone; b: pre-injection calcite-filled vein; c: injected sediment. Arrow: sense of injection. This injection occurred during the brecciation of siliciclastic layers close to the mudstone layer.

mudstone layers were truncated by ramps; this indicates a viscosity difference between these layers, the latter showing a greater competency than the former. Plastic behaviour of the marlstone and claystone is evidenced by some marlstone and claystone-filled veins in the sandstone and mudstone layers (b in Fig. 8 and a in Fig. 15). This indicates that marl and clay were still unlithified when the deformation occurred. These veins are equivalent to the calcite-filled veins described above, but they joined the bed surfaces (base or top), so that adjacent marl or clay could flow (upward and downward) into them, up to several decimetres from the bed surface. A layer-parallel fissility in the marlstone and claystone layers probably results from both compaction and tectonic layer-normal shortening.

Relationships of the microstructure development with strain and pore fluid pressure in the series

The microstructures described above are associated with the extensional ramps across the sandstone and mudstone layers and therefore probably result from internal deformation of these layers prior to the ramp initiation (Fig. 16). The development of a tensile rupture regime during this deformation implies that, locally: (i) σ_3 eff (the least principal effective stress) was layer-parallel and negative, and (ii) σ_1 eff $-\sigma_3$ eff (the differential stress) was small [theoretical values are σ_3 eff $= -T$ and σ_1 eff $-\sigma_3$ eff $=4T$, T being the tensile strength of the rock, according to Secor (1965), a in Fig. 12]. This may result from the fact that the initiation zones of the ramps are analogous to releasing overstep of faults, where mathematical simulations have shown that tensile rupture conditions can be realized (Segall & Pollard 1980; Liu 1983). The strain rate increase which may explain the vein-breccia transition may have been immediately prior to the bed rupture itself, as observed in many rock rupture experiments ['tertiary creep' (Price 1966)]. High pore pressure conditions may have assisted the rupture by shifting the Mohr circle leftward, according to the effective stress principle (Hubbert & Rubey 1960), but this was not a necessary condition, considering the evolution of the stress conditions prevailing in the overstep areas.

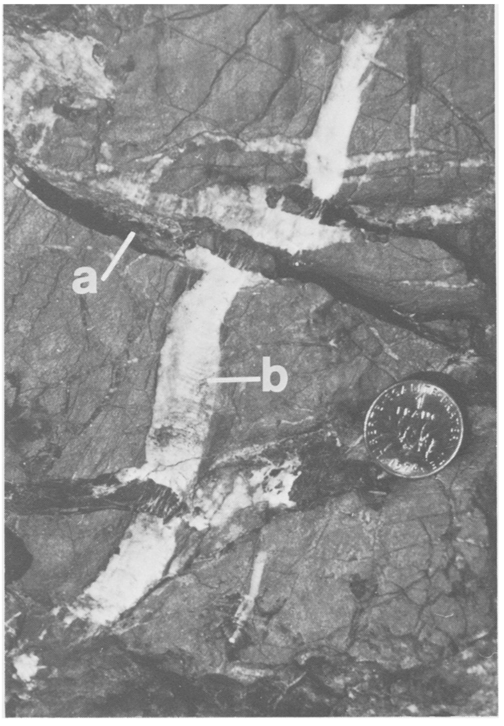

FIG. 15. Claystone-filled veins (a), partially emptied at outcrop, in sandstone. Note later calcite-filled veins (b), developed when the clay was no longer plastic enough to flow into the veins.

The bulk deformation of the succession basically consisted of layer-parallel decollements in the claystone and marlstone layers. This may result from high pore pressure conditions, reducing friction and thus facilitating movements along these low-angle shear planes (Hubbert & Rubey 1959). We can thus postulate the occurrence of high pore-pressure conditions which could not be easily constrained from the microstructure discussion. High pore-pressure could develop because in this incompletely lithified and dewatered succession, the marl and clay layers were barriers to the water escape. This assumption is consistent with the fact that the more deformed parts of the succession are the ones richer in marlstone and claystone. Therefore, the deformation was contemporaneous with compaction and water escape and it can also be considered as a local 'catastrophic' increment of these processes since it involved important mobilization of both the intergranular water and the grains.

Although the structures that we describe show some soft-sediment features, they do not correspond to slumps, i.e. intrabasinal, superficial syn-sedimentary gravity sliding (Gawthorpe & Clemmey 1985): (i) soft-sediment features are here restricted to very specific structures, the sediments being more lithified than in most classical slumps in basinal series; (ii) no evidence of syn-sedimentary structures can be found anywhere, i.e. no turbiditic deposits cover earlier structures. The structures are clearly post-sedimentary and must be regarded as classical tectonic features. Because of its relationship with lithification, this deformation can be referred to as syn-diagenetic.

Because of the local importance of the finite extension, this deformation stage cannot easily be expected to have occurred in a laterally confined area. It is more probable that it resulted from gravity spreading of the succession, probably associated with the first stages of the gravity-driven emplacement of the nappe. Deformation occurred in very superficial conditions: as indicated above, the Helminthoid Flysch was the last stratum deposited in the Tethyan Ocean and the nappe was emplaced as a submarine nappe, without having undergone any metamorphism. Its present thickness does not exceed 750 m, and it is generally much less than that. Its original thickness was greater, considering the local importance of extension, but it is unlikely that the structures described above developed to a depth of more than 2 or 3 km.

Diagenesis and deformation mechanisms post-dating the early bed ruptures

We have seen that where the grain cataclasis was weak, the deformed sandstone in the microfaults and breccia matrix was preferentially affected by later pressure-solution in calcite and by alteration by clay minerals. This probably resulted from easier fluid circulations (i.e. increased permeability) in the deformed sandstone than those in the undeformed one, due to a porosity increase resulting from: (i) destruction of early cements, and (ii) dilatancy during grain to grain movements. Therefore the immediate effect of the sandstone flow was to decompact the grains, but this in turn facilitated a stronger diagenesis in this deformed sandstone than in the undeformed one. In contrast, the sandstone in the highly cataclastic deformation band of Fig. 7 is less altered than the undeformed sandstone, probably because of a porosity (i.e. permeability) reduction resulting from the severe grain size reduction in this case.

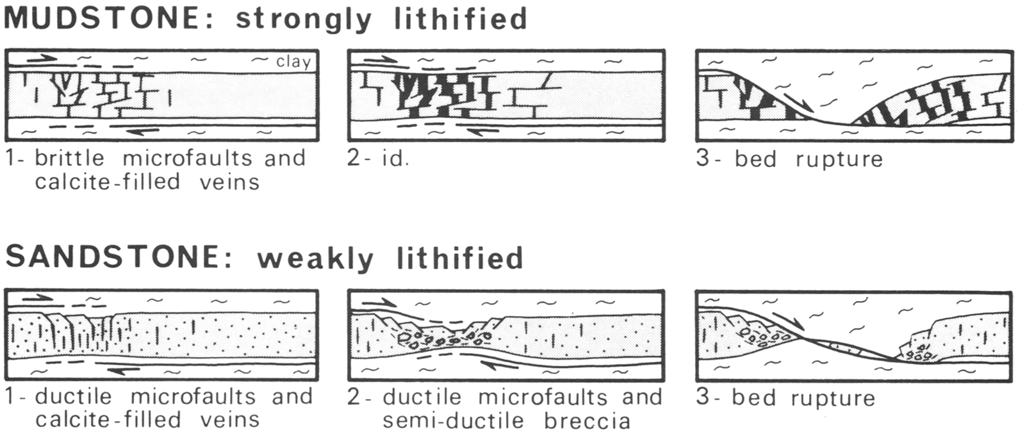

FIG. 16. Model of development of stratal disruption in the Helminthoid Flysch of the Autapie Nappe. The internal deformation of the mudstone and sandstone layers is related to the formation of extensional ramps joining decollements in the claystone or marlstone layers. The injection of siliciclastic grains inside a calcite-filled vein network in a mudstone layer presented in Fig. 15 occurred during stage 2, the sandstone and mudstone layers being adjacent in this case.

Later structures developed when all the sediments were strongly lithified and they emphasize the specificity of the structures described above. In the sandstone: (i) the slickensides exhibit grain abrasion and fibrous calcite and quartz crystallization, and (ii) calcite and quartz-filled vein opening induced grain breakage and no grain mobilization (no brecciation, e in Fig. 9); lithological changes of the sandstone did not control its behaviour any longer. In the marlstone and claystone, brittle behaviour is indicated by the presence of wide veins opened by boudinage, which exhibit calcite and quartz fill and which frequently remained partially empty; the marlstone and claystone were then no longer plastic enough to flow into the veins opened in the mudstone and sandstone layers (b in Fig. 15). Therefore, discrimination of the earlier and later stages of deformation by the determination of deformation mechanisms is a very useful tool for studying the structural evolution of the nappe.

Conclusion

We have presented an example of deformation resulting from extensional strain associated with the gravity driven emplacement of a submarine nappe. The deformation regimes and mechanisms were closely controlled by the nature and the state of lithification of the sediments, the strain rate and the occurrence of pore-water pressure gradients. The latter developed during tensile ruptures which may have resulted from horizontal confining relief in decollement overstep areas. Actual excess pore pressure cannot be proved, but was likely to occur in this water-saturated and marlstone and claystone-rich series. It could explain why the bulk deformation of the succession basically consisted of layer-parallel decollements. Detailed discussions have shown that the parameters controlling the deformation regimes and mechanisms can be appreciated, but that accurate determination of their respective influences remains speculative because they are likely to have varied, either together or separately, in both time and space through the nappe.

Some aspects of the sandstone, marlstone and claystone behaviour places such deformation in the category of 'soft-sediment' deformation. But there is also evidence that the sandstone was partially lithified and the mudstone strongly lithified. This deformation can thus be referred to as 'syndiagenetic' and represents an intermediate stage between classical soft-sediment deformation on the one side and rock deformation on the other. We have shown that this was a critical state for the sandstone, thus enabling an unusual deformation mechanism chronology to occur; partially ductile soft-sediment structures (brecciation) post-dating brittle, rock structures (calcite-filled veins). Therefore, our study sheds light on the progressive lithification of the various components of a basinal succession and emphasizes that: (i) a wide range of structures and associated deformation mechanisms exist among the structures referred to as 'soft-sediment' deformation, and (ii) soft-sediment deformation is not necessarily restricted to synsedimentary structures, but can also result from purely post-depositional, tectonic, deformation. Since the deformation involved intergranular water and grain mobilization and affected later fluid circulations in the poorly lithified sandstone, it can also be considered as a catastrophic increment of dewatering and compaction of the succession. Analogy can be made with convergent plate margins where tectonic deformation has been recognized to increase dewatering and compaction (Caron *et al.* 1982; Bray & Karig 1985; Fowler *et al.* 1985).

Deformation processes described here may be expected to be encountered at modern convergent margins: many accretionary prisms are composed of very similar partially lithified turbiditic succession and the importance of fluid overpressuring in the prism evolution is now well established (Von Huene & Lee 1982; Von Huene 1984; Shi & Wang 1985), either from seismic data (Biju-Duval *et al.* 1982; Westbrook & Smith 1983), core interpretation (Caron *et al.* 1982), *in situ* core measurement (Moore *et al.* 1982) and outcrop observations, both on land (Legget & Platt 1985) or during deep-sea dives (Suess & Massoth 1984; Boulègue *et al.* 1985). Specific deformation mechanisms resulting from these soft-sediment and high pore-pressure conditions are probably the cause of aseismic deformation in the prisms (Chen *et al.* 1982).

Analogy can also be made between the Autapie Nappe and these units, commonly referred to as 'melanges'. Cowan (1985) has recently pointed out that this term covers a wide range of geological units of sedimentary as well as tectonic origin, which developed under various conditions of pore-pressure and states of lithification of the sediments. He also postulated that melanges may develop in various tectonic settings, their common character being that they characterize convergent margins (see Cowan for specific bibliography). We have shown that, in our case: (i) accurate assumptions can be made concerning both the general tectonic setting and the deformation geometry and mechanisms, and (ii) discrimination of the various stages of deformation by determination of deformation mechanism changes is a useful tool in studying the structural evolution of this kind of structural unit.

ACKNOWLEDGEMENTS: This study was realized with the financial support of the *Centre National de la Recherche Scientifique*, France, as part of the programme 'A.T.P. Seismogénèse, Plis, Failles'. A. Etchecopar, M. Séguret and J. Mégard-Galli are greatly acknowledged for stimulating discussions and critical reviews of the manuscript, B. Sanche for making the thin-sections, M. F. Roch and J. Faure for help with the typewriting and M. Mareschal for improvement of the English.

References

AYDIN, A. 1978. Small faults formed as deformation bands in sandstone. *Pure App. Geophys,* **116**, 913–30.

—— & JOHNSON, A. M. 1983. Analysis of faulting in porous sandstones. *J. struct. Geol.* **5**–1, 19–31.

BIJU-DUVAL, B., LE QUELLEC, P., MASCLE, A., RENARD, V. & VALERY, P. 1982. Multibeam bathymetric survey and high resolution seismic investigations on the Barbados Ridge Complex (Eastern Caribbean): a key to the knowledge and interpretation of an accretionary wedge. *Tectonophysics,* **86**, 275–304.

BORG, J., FRIEDMAN, M., HANDIN, J. & HIGGS, D. V. 1960. Experimental deformation of St. Peter sand: a study of cataclastic flow. *In:* GRIGGS, D. & HANDIN, J. (eds) *Rock Deformation.* Geol. Soc. Amer. Mem. no. 79, 133–91.

BOULÈGUE, J., LE PICHON, X. & IIYAMA, J. T. 1985. Prévision des tremblements de terre dans la région du Tokai (Japon). *Comptes Rendus des Séances de l'Académie des Sciences, Paris,* **301 (Série II)**–16, 1217–9.

BRAY, C. J. & KARIG, D. E. 1985. Porosity of sediments in accretionary prisms and some implications for dewatering processes. *J. geophys. Res.* **90**–B1, 768–78.

CARON, C., HESSE, R., KERCKHOVE, C., HOMEWOOD, P., VAN STUIJVENBERG, J., TASSE, N. & WINKLER, W. 1981. Comparaison préliminaire des flyschs à Helminthoides sur trois transversales des Alpes. *Ecl. Geolog. Helvet.* **47**–2, 369–78.

CARSON, B. H., VON HUENE, R. & ARTHUR, M. 1982. Small scale deformation structures and physical properties related to convergence in Japan trench slope sediments. *Tectonics,* **1**(3), 277–302.

CHEN, A. T., FROHLICH, C. & LATHAM, G. 1982. Seismicity of the forearc marginal wedge (accretionary prism). *J. geophys. Res.* **87**–B5, 3679–90.

COWAN, D. S. 1982. Deformation of partly dewatered and consolidated Franciscan sediments near Piedras Blancas Point, California. *In:* LEGGETT, J. K. (ed) *Trench-Forearc Geology: Sedimentation and Tectonics on Modern and Ancient Active Plate Margins.* Spec. Publ. geol. Soc. London, **10**, 439–57.

——, 1985. Structural styles in Mesozoic and Cenozoic melanges in the Western Cordillera of North America. *Geol. Soc. America Bull.* **96**, 451–62.

DEBELMAS, J. 1975. Réflexions et hypothèses sur la paléogéographie crétacée des confins alpino-apenniniques. *Bull. Soc. Géol. de France*. (7), **XVII**-6, 1002–12.

—— & KERCKHOVE, C. 1973. Large gravity nappes in the French-Italian and French-Swiss Alps. *In:* DE JONG, K. A. & SCHOLTEN, R. (eds) *Gravity and Tectonics*. 189–200.

DE SITTER, L. U. 1966. *Structural Geology*. McGraw-Hill, New York.

DUNN, D. E., LAFOUTAIN, L. J. & JACKSON, R. E. 1973. Porosity dependence and mechanisms of brittle fracture in sandstones. *J. geophys. Res.* **78**–14, 2403–17.

FITCHES, W. R. & MALTMAN, A. J. 1978. Conference report: Deformation of soft sediments. *J. geol. Soc. London*, **135**–2, 245–51.

FOWLER, S. R., WHITE, R. S. & LOUDEN, K. E. 1985. Sediment dewatering in the Mackran accretionary complex. *Earth planet. Sci. Lett.* **75**, 427–38.

FRIEDMAN, M., HUGMAN, R. H. H. III & HANDIN, J. 1980. Experimental folding of rocks under confining pressure, Part VIII—Forced folding of unconsolidated sand and of lubricated layers of limestone and sandstone. *Geol. Soc. America Bull.* **91**, 307–12.

GAWTHORPE, R. L. & CLEMMEY, H. 1985. Geometry of submarine slides in the Bowland Basin and their relation to debris flows. *J. geol. Soc. London*, **142**, 555–66.

HANDIN, J., HAGER, R. V. Jr, FRIEDMAN, M. & FEATHER, J. N. 1963. Experimental deformation of sedimentary rocks under confining pressure: pore pressure test. *Amer. Assoc. Petrol. Geol. Bull.* **47**–5, 717–55.

HESSE, R. & BUTT, A. 1976. Paleobathymetry of Cretaceous turbidite basins of the east Alps relative to the calcite compensation level. *J. Geol.* **84**, 505–33.

HOMEWOOD, P. & CARON, C. 1982. Flysch of the western Alps. *In:* HSÜ, K. J. (ed) *Mountain Building Processes*. 2–2, 157–68. Academic Press, London.

HSÜ, K. J. 1974. Melanges and their distinction from olistostromes. *In:* DOTT, R. M. J. & SHAVER, R. H. (eds) *Modern and Ancient Geosynclinal Sedimentation*. Spec. Publ. Soc. Econ. Paleont. Mineral. **19**, 321–33.

HUBBERT, M. K. & RUBEY, W. W. 1959. Role of fluid pressure in mechanics of overthrust faulting, I: mechanics of fluid-filled porous solids and its application to overthrust faulting. *Geol. Soc. Amer. Bull.* **70**–2, 115–66.

—— & RUBEY, W. W. 1960. Role of fluid pressure in mechanics of overthrust faulting—reply. *Geol. Soc. Amer. Bull.* **71**–5, 611–28.

—— & WILLIS, D. G. 1957. Mechanics of hydraulic fracturing. *Trans. Amer. Inst. Mech. Engineers*, **210**, 153–68.

HUENE, R. VON, 1984. Structural diversity along modern convergent margins and the role of overpressured pore fluids in subduction zones. *Bull. Soc. Géol. France*, **7**, XXVI–2, 207–19.

—— & LEE, H. 1982. The possible significance of pore fluid pressures in subduction zones. *In:* WATKINS, J. S. & DRAKE, C. L. (eds) *Studies in Continental Margin Geology*. Amer. Assoc. Petrol. Geol. Mem. no. 34, 781–91.

KERCKHOVE, C. 1969. La 'zone du Flysch' dans les nappes de l'Embrunais-Ubaye (Alpes occidentales). *Géol. Alpine*, **45**, 5–204.

——, BEBELMAS, J. & COCHONAT, P. 1978. Tectonique du soubassement parautochtone des nappes de l'Embrunais-Ubaye sur leur bordure occidentale, du Drac au Verdon. *Géol. Alpine*, **54**, 67–82.

——, CARON, C., CHAROLAIS, J. & PAIRIS, J.-L. 1981. Panorama des séries synorogéniques des Alpes occidentales. *In:* AUTRAN, A. & DERCOURT, J. (eds) *Evolutions Géologiques de la France*. Bur. Rech. Géol. Min. Mém. no. 17, 234–55.

LAVILLE, E. & PETIT, J. P. 1984. Role of synsedimentary strike-slip faults in the formation of Moroccan Triassic basins. *Geology*, **12**, 424–7.

LEGGETT, J. K. & PLATT, J. 1985. Soft-sediment deformation and mud diapirism, Makran accretionary prism, paper presented at the conference on 'Deformation Mechanisms in Sediments and Sedimentary Rocks', University College London, April 15–17.

LIU, X. 1983. *Perturbations des contraintes liées aux structures cassantes dans les calcaires fins du Languedoc. Observations microtectoniques et simulations mathématiques*. (Unpublished thesis) University of Montpellier, France.

LOWE, D. R. 1976. Subaqueous liquified and fluidized sediment flows and their deposits. *Sedimentology*, **23**, 285–308.

MALAVIEILLE, J., LACASSIN, R. & MATTAUER, M. 1984. Signification tectonique des linéations d'allongement dans les Alpes occidentales. *Bull. Soc. Géol. France*, **7**, XXVI–5, 895–906.

MALTMAN, A. 1984. On the term 'soft-sediment deformation'. *J. struct. Geol.* **6**–5, 589–92.

MANDL, G., DE JONG, L. M. J. & MALTHA, A. 1977. Shear zones in granular material. *Rock Mechanics*, **9**, 95–144.

MERLE, O. & BRUN, J. P. 1984. The curved translation path of the Parpaillon Nappe (French Alps). *J. struct. Geol.* **6**–6, 711–9.

MOORE, C. J., BIJU-DUVAL, B. & DSDP Leg 78A Scientific party. 1982. Offscraping and underthrusting of sediments at the deformation front of the Barbados Ridge: Deep Sea Drilling Project Leg 78A. *Geol. Soc. Amer. Bull.* **93**, 1065–77.

PETIT, J. P. & LAVILLE, E. Morphology and microstructure of hydroplastic slickensides. *This volume*.

——, PROUST, F. & TAPPONNIER, P. 1983. Critères de sens de mouvement sur les miroirs de failles en roches non calcaires. *Bull. Soc. géol. France*, **7**, XXV–4, 589–608.

PRICE, N. J. 1966. *Fault and Joint Development in Brittle and Semi-Brittle Rock*. Pergamon Press, Oxford.

SEGALL, P. & Pollard, D. O. 1980. Mechanics of discontinuous faults. *J. geophys. Res.* **85**–B8, 4337–50.

SAGRI, M. 1979. Upper Cretaceous carbonate turbidites of the Alps and Apennines deposited below the calcite compensation level. *J. sed. Petrol.* **49**–1, 23–8.

SECOR, D. T. 1965. Role of fluid pressure in jointing. *Amer. J. Sci.* **263**, 633–46.

SHI, Y. & WANG, C. Y. 1985. High pore pressure generation in sediments in front of the Barbados Ridge complex. *Geophys. Res. Lett.* **12**–11, 773–6.

SUESS, E. & MASSOTH, G. J. 1984. Evidence for the venting of pore waters from subducted sediments in the Oregon continental margin. *EOS Trans. Amer. Geophys. Union*, **65**–45, 1089.

TERZAGHI, K. W. 1943. *Theoretical Soil Mechanics*. Wiley, New York.

TRICART, P. 1984. From passive margin to continental collision: a tectonic scenario for the western Alps. *Amer. J. Sci*, **284**, 97–120.

UNDERHILL, J. R. & WOODCOCK, N. H. Faulting mechanisms in high-porosity sandstones; Permo-Triassic, Arran, Scotland. *This volume*.

WESTBROOK, G. K. & SMITH, M. J. 1983. Long decollements and mud volcanoes: evidence from the Barbados Ridge Complex for the role of high pore-fluid pressure in the development of an accretionary complex. *Geology*, **11**, 279–83.

P. LABAUME, Laboratoire de Tectonique (u.a. CNRS 266), Université des Sciences et Techniques du Languedoc, Place E. Bataillon, 34060 Montpelier Cedex, France.